NeuroImage: Clinical 25 (2020) 102133

Contents lists available at ScienceDirect

NeuroImage: Clinical

journal homepage: www.elsevier.com/locate/ynicl

Organization of the commissural fiber system in congenital and late-onset blindness

Carlo Cavaliere[a,b,*], Marco Aiello[a], Andrea Soddu[c], Steven Laureys[b], Nina L Reislev[d], Maurice Ptito[e,f,g], Ron Kupers[e,g,h,**]

[a] IRCCS SDN, Via E. Gianturco 113, 80143 Naples, Italy
[b] GIGA-Consciousness - Coma Science Group, GIGA-Research and Neurology Department, University and University Hospital of Liège, Liège, Belgium
[c] Brain and Mind Institute, The Department of Physics and Astronomy, University of Western Ontario London, ON, Canada
[d] Danish Research Centre for Magnetic Resonance, Centre for Functional and Diagnostic Imaging and Research, Copenhagen University Hospital Hvidovre, 2650 Hvidovre, Denmark
[e] Ecole d'Optométrie, Université de Montréal, Montréal, Québec, Canada
[f] Department of nuclear Medicine, University of Southern Denmark, Odense, Denmark
[g] BRAINlab, Institute of Neuroscience, Panum Institute, Faculty of Health and Medical Sciences, University of Copenhagen, Nørre Allé 10, 2200 Copenhagen,Denmark
[h] Institute of Neuroscience, Université Catholique de Louvain, Brussels, Belgium

ARTICLE INFO

Keywords:
Blindness
Commissural pathways
Corpus callosum
Anterior commissure
Spherical deconvolution tractography
Resting-state fMRI

ABSTRACT

We investigated the effects of blindness on the structural and functional integrity of the corpus callosum and the anterior commissure (AC), which together form the two major components of the commissural pathways. Twelve congenitally blind (CB), 15 late blind (LB; mean onset of blindness of 16.6 ± 8.9 years), and 15 matched normally sighted controls (SC) participated in a multimodal brain imaging study. Magnetic resonance imaging (MRI) data were acquired using a 3T scanner, and included a structural brain scan, resting state functional MRI, and diffusion-weighted imaging. We used tractography to divide the AC into its anterior (aAC) and posterior (pAC) branch. Virtual tract dissection was performed using a deterministic spherical deconvolution tractography algorithm. The corpus callosum was subdivided into five subregions based on the criteria described by Witelson and modified by Bermudez and Zatorre. Our data revealed decreased fractional anisotropy of the pAC in CB and LB compared to SC, together with an increase in the number of streamlines in CB only. In addition, the AC surface area was significantly larger in CB compared to SC and LB, and correlated with the number of streamlines in pAC (rho = 0.55) and tract volume (rho = 0.46). As for the corpus callosum, the splenial part was significantly smaller in CB and LB, and fewer streamlines passed through it. We did not find group differences in functional connectivity of cortical areas connected by fibers crossing any of the five callosal subregions. The present data suggest that the two main components of the commissural system undergo neuroplastic changes, irrespective of the age of onset of blindness, although the alterations observed in the AC are more important in congenital than late-onset blindness.

Introduction

There is now ample evidence that visual deprivation strongly modulates brain structure and function (Bavelier and Neville, 2002; Noppeney 2007; Ptito et al., 2008; Kupers et al., 2011; Heine et al., 2015). These plastic rearrangements even occur outside the visually deprived occipital cortex, and include cortical, subcortical and white matter structures not directly related to visual processing (Kupers and Ptito, 2014; Desgent and Ptito 2012). For instance, several authors have reported differences in hippocampal subfields (Chebat et al., 2007; Fortin et al., 2008), anterior insula (Liu et al., 2017), corticospinal tract (Yu et al., 2007) and the tonotopic region of the auditory cortex (Elbert et al., 2002; Stevens and Weaver, 2009) of blind compared to sighted subjects.

Structural changes of the corpus callosum following visual deprivation have been well studied in both animal models (Lund and

* Corresponding author at: NAPLab, IRCCS SDN Istituto di Ricerca Diagnostica e Nucleare, Via E. Gianturco 113, 80143 Naples, Italy.
** Corresponding author at: BRAINlab, Institute of Neuroscience, Panum Institute, Faculty of Health and Medical Sciences, University of Copenhagen, Nørre Allé 10, 2200 Copenhagen,Denmark
E-mail addresses: ccavaliere@sdn.it (C. Cavaliere), kupers@sund.ku.dk (R. Kupers).

https://doi.org/10.1016/j.nicl.2019.102133
Received 3 June 2019; Received in revised form 4 December 2019; Accepted 13 December 2019
Available online 14 December 2019

Mitchell 1979; Frost and Moy 1989; Berman and Payne 1983; Tremblay et al., 1987) and in human models of blindness (Ptito et al., 2008; Tomaiuiolo et al., 2014; Leporé et al., 2010; Levin et al., 2010; Bridge et al., 2009; Bock et al., 2013; Reislev et al., 2016). Collectively, these studies have shown alterations in the corpus callosum following visual deprivation from birth (reviewed in Kupers and Ptito, 2014). Although all studies concur on a volume reduction of the splenium, i.e. the posterior part of the corpus callosum, results regarding the other portions of the corpus callosum are inconclusive (Ptito et al., 2008; Tomaiuolo et al., 2014; Leporé et al., 2010; Levin et al., 2010; Bridge et al., 2009; Bock et al., 2013). For example, some authors have found an enlargement of the genu, the anterior portion of the corpus callosum (Ptito et al., 2008; Lepore et al., 2010), others an enlargement of the isthmus and the posterior part of the body (Tomaiuolo et al., 2014); still others found no changes at all in the anatomical organization of the corpus callosum (Bock et al., 2013).

To the best of our knowledge, no studies have investigated the effects of blindness on the anterior commissure (AC) which is the second main component of the commissural system (Lamantia and Rakic, 1990). There is evidence that axons originating from the occipital and the inferior temporal cortices send projections through the AC (Di Virgillio et al., 1999), suggesting that blindness may affect its structural and functional organization. The functional importance of the AC in visual functions has been highlighted in various animal and human studies of callosal splits or callosal agenesis (reviewed in Lassonde and Jeeves, 1994) showing that the AC becomes enlarged and can facilitate interhemispheric transfer of visual information in the presence of corpus callosum deficiencies. For example, patients with callosal agenesis who show an enlarged AC have a normal interhemispheric transfer of visual information, suggesting that the AC may compensate for the absence of the corpus callosum (Guenot, 1998; Brown et al., 1999; Barr and Corballis, 2002; Bayard et al., 2004). In addition, acallosal mice have a significantly larger number of axons in the AC compared to controls (Livy et al., 1997).

The primary aim of the present study was to study purported anatomical modifications of the AC following congenital and late-onset visual deprivation, thereby combining T1 structural markers with resting-state fMRI and diffusion weighted imaging (DWI) data. In order to better resolve fiber resolution in crossing points that mainly affects commissural bundles, we used a tractography algorithm based on deterministic spherical deconvolution which gives improved results for *in vivo* virtual dissection of these pathways (Dell'Acqua et al., 2013). A secondary aim was to compare changes in the organization of the corpus callosum in congenitally blind (CB) and late-onset blind (LB) subjects.

Material and methods

Study participants

We included 12 CB (mean age: 42 ± 13 y), 15 LB (mean age 52 ± 15 y) and 15 normal sighted control (SC) subjects (mean age 46 ± 13 y). The three groups were matched for gender, age, and handedness. Mean onset of blindness in the LB group was 16.6 ± 8.9 y (range: 6 - 60 y). All blind subjects suffered from blindness caused by bilateral peripheral damage to the visual system causing total blindness. Retinopathy of prematurity (ROP) was the main cause of blindness, while one subject suffered from both ROP and glaucoma (Table 1). CB subjects were classified as such, based on self-reports of medical history and etiology. The ethics committee for the city of Copenhagen and Frederiksberg (Denmark) had approved the experimental procedures and all participants gave their informed consent.

MRI data acquisition

Brain MRIs were acquired using a 3 Tesla Siemens Verio MRI system (Siemens, Erlangen, Germany) equipped with a 32-channel head coil. Structural scans were acquired using a 3D T1-weighted MPRAGE sequence (TE = 2.32 ms, TR = 1900 ms, flip angle = 9°, isotropic 0.93 mm^3 voxels). Functional images were acquired using an EPI sequence (280 volumes, TR = 2150 ms, TE = 26 ms, flip angle = 78°, FOV = 192mm^2, 64 × 64 matrix, 43 axial slices of 4 mm) at rest, with eyes closed (resting state fMRI, rsfMRI). Head motion was restricted by placement of comfortable padding around the participant's head. Finally, diffusion-weighted images (DWIs) were acquired using a twice-refocused spin-echo sequence with a 2.33 mm^3 isotropic resolution in 61 non-collinear directions (*b*-value of 1500 s/mm^2). Moreover, to improve signal-to-noise ratio (SNR) in the tensor estimation (Jones et al., 1999; Chen et al., 2015), ten non-diffusion-weighted volumes were acquired and averaged to obtain a reliable b0 map. A set of reversed phase-encoded $b = 0$ images was also acquired for pre-processing purposes.

Manual segmentation of the corpus callosum and the AC

In order to be more consistent with manual segmentation procedures and to reduce possible bias due to brain tilting, in a first step we aligned each pre-processed subject's T1 imagemanually by positioning it along the anterior-posterior commissure plane (AC-PC line) and rotating it such that the septum pellucidum and at least a large part of the falx were visible in the sagittal plane (Tomaiuolo et al., 2014). Next, we performed segmentation and tractography reconstructions in the subject individual space.

The corpus callosum was defined using the mid-sagittal MRI slice in which the septum pellucidum and the falx were simultaneously visible, considering the peri-callosal sulcus for the dorsal and rostral boundaries, whereas the third ventricle and the cisterna superior for the ventral boundary. A trained neuroradiologist (CC) manually drew the minimum rectangle circumscribing the corpus callosum in the mid-sagittal plane. Next, four lines perpendicular to the longest side of the minimum rectangle subdivided the corpus callosum into five contiguous sub-regions, covering 33, 17, 17, 13 and 20% of its total length, respectively(Tomaiuolo et al., 2014). This division resulted in the following contiguous subregions along the rostro-caudal direction: a) the anterior third of the corpus callosum, including the rostrum, the genu, and the rostral body; b) the anterior mid-body; c) the posterior mid-body; d) the isthmus; and e) the splenium (Fig. 1). This division is based on a modification of the original Witelson, 1989 segmentation of the corpus callosum in seven segments, but whereby the anterior sections of the corpus callosum are kept together (Bermudez and Zatorre, 2001). The five callosal subregions were estimated in terms of area (mm^2) and were used as seed-points for the tracking algorithm (Trackvis; Ruopeng Wang, Van J. Wedeen, TrackVis.org, Martinos Center for Biomedical Imaging, Massachusetts General Hospital) (Wedeen et al., 2008).

The AC was defined using the mid-sagittal MR image (Mai et al., 1997) where it crosses the midline as a compact cylindrical bundle between the anterior and posterior columns of the fornix, beneath the septum pellucidum and the anterior to the third ventricle (Dejerine, 1895). The AC area was estimated (in mm^2) and used for tractography reconstruction. The AC was divided into an anterior (aAC) and posterior (pAC) branch, using a VOI to VOI approach in Trackvis (Fig. 1).

MRI data processing

We used ExploreDTI for data preprocessing and spherical deconvolution-based tractography (Catani et al., 2017). The diffusion-weighted (DW) images were corrected for subject motion and eddy-current-induced distortions, after which the b-matrix was reoriented to provide a more accurate estimate of diffusion tensor orientations (Leemans and Jones 2009). Spherical deconvolution was calculated applying the damped version of the Richardson–Lucy algorithm with a

Table 1
Demographic data participants.

Overall Sample			
Variable	***Blind subjects***&&(n or mean ± SD)	***Healthy controls***&&(n or mean ± SD)	***Group comparison***
Age	48 ± 15 y	46 ± 12 y	$p = 0.89$
Sex (male/female)	14/12	8/7	$p = 0.97$
Handedness (right/left)	24/2	14/1	$p = 0.9$
Blind subgroups			
Variable	**Congenitally blind**&&(n or mean ± SD)	**Late blind**&&(n or mean ± SD)	***Group comparison***
Age	42 ± 14 y	53 ± 15 y	$p = 0.10$
Onset of blindness	birth	17 ± 9 y	
Sex (male/female)	7/5	7/7	$p = 0.67$
Pathogenesis			
Retinopathy of prematurity	11	10	
Glaucoma	1	4	
Unknown	1		

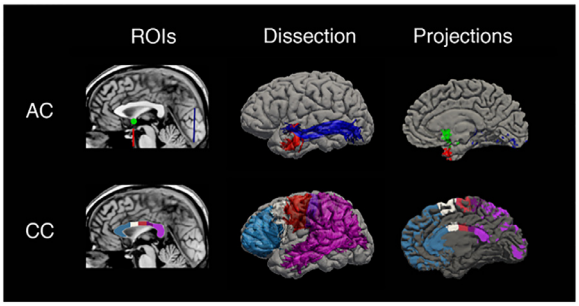

Fig. 1. *Analysis workflow for AC and corpus callosum commissural pathways.* The left column shows a midline sagittal T1 slice indicating the AC and the five segments of the corpus callosum. The middle column shows a lateral view of a brain volume rendering with superimposed streamlines as revealed by tractography; the upper row shows the anterior (red) and posterior (blue) branches of the AC, whereas the lower row shows corpus callosum fibers originating from the anterior third (light blue), anterior mid-body (white), posterior mid-body (red), isthmus (violet) and splenium (purple). The right column shows cortical projections for each commissural segment as determined by functional connectivity analysis. (For interpretation of the references to color in this figure legend, the reader is referred to the web version of this article.)

fiber response parameter of $\alpha = 1.5$, 200 algorithm iterations, an ALFA value of 2, threshold parameters of 0.04, and geometrical regularization parameters of 8 (Dell'Acqua et al., 2013). Fiber orientation estimates were obtained by selecting the orientation corresponding to the peaks (local maxima) of the fiber orientation distribution (FOD) profiles. Whole brain tractography was run on the diffusion datasets using a step size of 1 mm with a limit set to display only streamlines between 15 and 400 mm in length. The Euler algorithm was used to follow the orientation vector of least curvature (angle threshold of 60°), thus allowing to track through crossing fibers (Dell'Acqua et al., 2013). All spherical deconvolution and tractography analyses were performed using StarTrack software (http//www.mr-startrack.com/).

The rsfMRI data were pre-processed using DPABI 4.0 (Chao-Gan and Yu-Feng, 2010; Aiello et al., 2015; Cavaliere et al., 2016), a Matlab (Mathworks Inc.) toolbox containing libraries for fMRI analysis that rely on the Statistical Parametric Mapping 8 package (SPM8, Wellcome Department of Neurology, London UK (Friston and Frith, 1995). The three initial volumes were discarded to avoid T1 saturation effects. The first 10 time points were removed to avoid non-equilibrium effects of magnetization. The remaining 230 volumes were corrected for slice timing effects; motion correction was performed by aligning all volumes to the first time point (Friston and Frith, 1995). Runs in which head motion exceeded 3.0 mm and/or 3.0° were excluded from the analysis. In order to remove BOLD signal fluctuations unrelated to neuronal activity, the white matter and cerebrospinal fluid mean signals were regressed out as nuisance variables (Zuo et al., 2013). To take into account signal drifts arising from scanner instability or other possible causes, linear trend effects were removed from each voxel's time course.

Imaging post-processing

The FA values were calculated by averaging across all voxels in the tract. Tract volume was calculated by multiplying the number of voxels containing reconstructed streamlines with the voxel size (2.33 mm^3) (Reich et al., 2006).

Functional connectivity between regions structurally connected by AC and corpus callosum segments was estimated by considering the intersection between the endpoints of the segment for each hemisphere and the relative parcel of grey matter as pair of regions of interest (ROI). Therefore, we calculated Pearson correlations between the preprocessed rsfMRI time courses as obtained by averaging across the ROIs belonging to each commissural subregion (mean BOLD correlation). Network graphs were created using a circular layout function in Matlab (Mathworks Inc.).

Statistical analysis

A chi-square test was applied for comparison of qualitative variables (e.g. sex, handedness). Group differences between the DTI parameters and the Pearson correlation coefficients of blind and sighted participants were assessed by means of a two-sample *t*-test as implemented in SPM. A one-way analysis of variance (ANOVA) was performed for DTI parameters of the five callosal sub-regions and in case of significance, a Bonferroni correction was used for multiple comparisons, with p-values < 0.01 considered as statistically significant. Data are presented as mean ± SD.

Results

Differences in structural and functional connectivity of the AC in blind subjects

The AC midline area was significantly larger in CB (8.54 ± 2.10 mm^2) compared to LB (5.97 ± 1.59 mm^2; $p = 0.002$) and SC (6.42 ± 1.34 mm^2; $p = 0.007$) (Fig. 2A). CB showed a significant increase in the number of streamlines in pAC (131.92 ± 53.5) compared to SC (75.33 ± 72.62; $p = 0.007$) and LB (82.75 ± 41.59; $p = 0.01$) (Fig. 2B), without differences in tract volume (Figs. 2C and 3). In addition, the mean FA of the pAC was significantly reduced in both CB (0.24 ± 0.03; $p < 0.001$) and LB (0.24 ± 0.03; $p < 0.001$) compared to SC (0.28 ± 0.03) (Figs. 2D and 3). There were no significant differences between CB and LB for the other tractography parameters extracted, neither for the pAC nor the aAC projections (Table 2). When combining the results of all participants together, AC surface area correlated significantly with both the number of streamlines (rho = 0.55, $p < 0.001$, Fig. 2E) and tract volume (rho = 0.46,

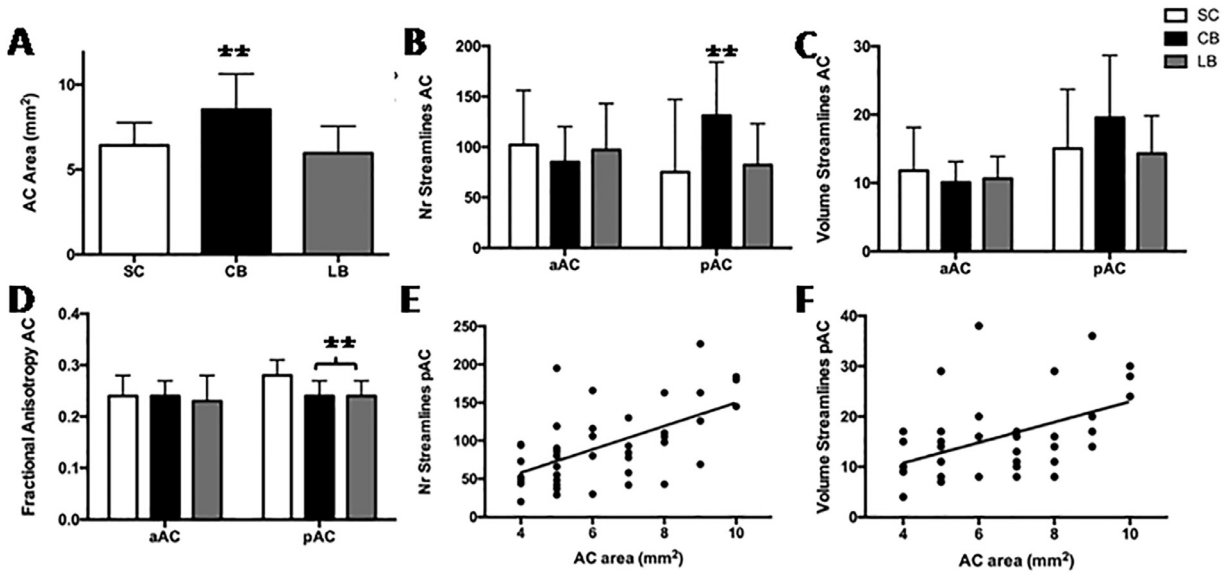

Fig. 2. *Tractography analysis of the pAC and aAC.* (A)The area of the AC as measured on the mid sagittal plane, (B) number of streamlines, (C) tract volume and (D) fractional anisotropy for the anterior (aAC) and posterior (pAC) branch of the AC. Scatter plots show correlation between AC area with number of streamlines (E) and tract volume (F) of the pAC. **, $p < 0.01$.

$p = 0.002$, Fig. 2F) of pAC, but not of aAC.

We did not detect group differences in functional connectivity of cortical areas connected by fibers composing the aAC and pAC ($p = 0.51$) (Table 2, Fig. 4).

Changes in structural and functional connectivity of the corpus callosum in blind subjects

There were no significant group differences in total corpus callosum midline surface area (CB: 805.5 ± 61 mm^2, LB: 794.5 ± 69 mm^2, SC: 881.25 ± 63.75 mm^2). Looking at subregional areas, the splenium surface area was significantly smaller in both CB (215 ± 32.5 mm^2) and LB (215.75 ± 38 mm^2) compared to SC (257.75 ± 53 mm^2) ($p = 0.01$ for both comparisons) (Fig. 5A). No significant group differences were found for any of the four other subregions.

We measured a significant reduction in the number of streamlines in the splenium of CB and LB compared to SC (SC: 2415 ± 623; CB: 1653 ± 397, $p < 0.001$; LB: 1706 ± 518, $p = 0.003$) (Figs. 3 and 5B). Similarly, we found a significant reduction in tract volume crossing the splenium region of CB (80.83 ± 21.34) and LB (75 ± 13.34) compared to SC (105.82 ± 24.22; $p = 0.003$ and 0.009, respectively) (Figs. 3 and 5C). When combining the results of all participants together, the splenium surface correlated significantly with both the number of streamlines (rho = 0.63, $p < 0.001$, Fig. 5D) and the tract volume (rho = 0.59, $p < 0.001$, Fig. 5E) passing through it. There were no significant group differences in tract volume, number of streamlines, FA, mean and axial diffusivity in the anterior third, anterior mid-body, posterior mid-body and isthmus. There were also no group differences in functional connectivity of cortical areas connected by fibers crossing the five callosal subregions ($p = 0.56$) (Table 3, Fig. 4).

Discussion

The present study shows that the two major branches of the commissural system, the AC and the corpus callosum, undergo neuroplastic changes following both congenital and late-onset blindness. More specifically, both CB and LB showed a decrease in FA of the pAC which went together with an increase in the number of streamlines for this area in CB only. This finding was paralleled by an increase of the AC area in CB and a positive correlation between AC area and the number of streamlines in pAC and tract volume for all participants. At the same time, using a different methodology, we confirm and extend previous

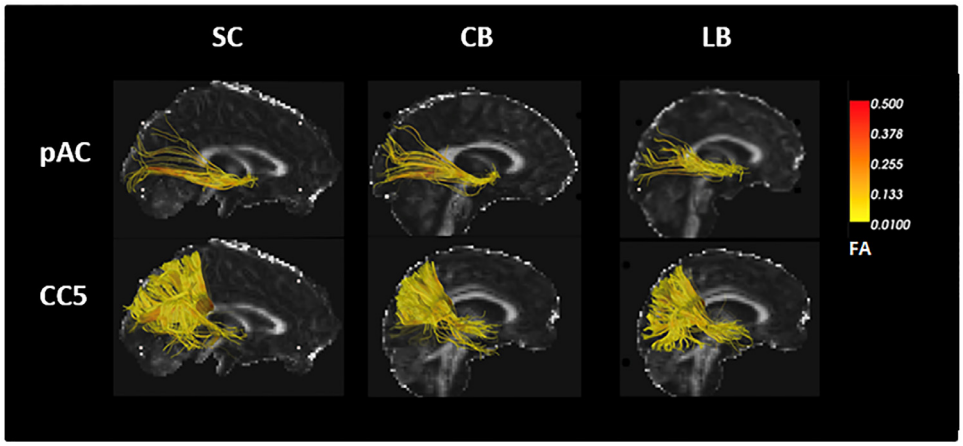

Fig. 3. *Tractography reconstructions for pAC and CC5 in a representative SC,CB and LB participant.* Tracts area represented in scalar colours, corresponding to relative FA values along the streamlines.

Table 2
Tract-specific measurements and functional connectivity analysis of the two segments of the anterior commissure.

Segments	Measurements	SC&&(mean + SD)	CB&&(mean ± SD)	LB&&(mean ± SD)	CB vs SC&&p value	LB vs SC&&p value	CB vs LB&&p value
Anterior	Streamlines	102.2 ± 124.83	85.33 ± 35.76	97.64 ± 46.4	0.62	0.9	0.45
	Volume	11.8 ± 8.35	7.08 ± 3.06	9.64 ± 3.25	0.29	0.62	0.05
	FA	0.24 ± 0.04	0.24 ± 0.03	0.23 ± 0.05	0.87	0.5	0.56
	MD	0.7 ± 0.06 x (10–3)	0.7 ± 0.05 x (10–3)	0.7 ± 0.1 x (10–3)	0.76	0.8	0.65
	AD	0.9 ± 0.08 x (10–3)	0.9 ± 0.1 x (10–3)	0.9 ± 0.1 x (10–3)	0.52	0.59	0.94
	Mean BOLD correlation	0.92 ± 0.09	0.92 ± 0.08	0.87 ± 0.09	0.75	0.72	0.8
Posterior	Streamlines	75.33 ± 42.62	131.92 ± 53.5	82.75 ± 41.59	0.007*	0.65	0.01
	Volume	15.04 ± 8.66	19.57 ± 9.09	14.32 ± 5.51	0.2	0.79	0.09
	FA	0.28 ± 0.03	0.24 ± 0.03	0.24 ± 0.03	0.001*	0.001*	0.57
	MD	0.7 ± 0.04 x (10–3)	0.8 ± 0.1 x (10–3)	0.8 ± 0.1 x (10–3)	0.05	0.32	0.79
	AD	0.9 ± 0.05 x (10–3)	1 ± 0.1 x (10–3)	1 ± 0.1 x (10–3)	0.37	0.79	0.76
	Mean BOLD correlation	0.9 ± 0.03	0.91 ± 0.08	0.9 ± 0.08	0.72	0.84	0.7

Numbers represent means ± SD. *Indicates values that survive Bonferroni correction for multiple comparisons. FA = fractional anisotropy; MD = mean diffusivity; AD = axial diffusivity.

reports of structural alterations of the corpus callosum in blind individuals, by demonstrating that tract volume of fibers crossing the splenium is reduced in both CB and LB.

Neuroplastic changes of the anterior commissure in blindness

It has been well described that in case of complete sectioning of the corpus callosum, as in split-brain, or when absent from birth (agenesis of the corpus callosum), other commissures like the AC reorganize to insure interhemispheric transfer of visual information (Ptito and Leporé, 1983; Barr and Corballis, 2002), even between primary visual cortical areas (van Meer et al., 2016). The present data show that the AC also undergoes neuroplastic changes following congenital or late onset blindness. Indeed, we measured an increase of the AC area in CB, and a decrease in FA in the posterior part of the AC tracts in both CB and LB, combined with an increase in the number of streamlines in CB. Previous studies investigating brain plasticity in other physiological and pathological conditions have shown an increase in the number of streamlines associated with a reduction of fractional anisotropy values (Imfeld et al., 2009; Hänggi et al., 2010; Giacosa et al., 2016). From a microstructural perspective, these findings could be due to two different processes typically associated with brain plasticity, i.e. fiber sprouting and neurogenesis. Both processes are associated with an increased number of streamlines that however are not fully covered by myelin, leading to a reduced longitudinal fractional anisotropy.Here, AC streamlines changes occurred without an associated alteration in tract volume of the pAC. The latter negative finding might be due to the small size of the tract compared to our DWI image resolution. Nevertheless, we found a non-significant trend to increased tract volume in the CB group, paralleling the findings derived from the number of streamlines. Moreover, both the number of streamlines and the pAC tract volume were positively correlated with the AC area, as was also demonstrated in other studies (Patel et al., 2010). Although adaptive neuroplastic changes have traditionally been associated with increases in FA, there are other reports that improvement in performance in professional musicians and dancers may be linked with decreases in FA (Imfeld et al., 2009; Hänggi et al., 2010; Giacosa et al., 2016).

It is known that the majority of fibers of the aAC connect the olfactory bulb, anterior perforated substance, and anterior olfactory nucleus, whereas the pAC links the amygdala, hippocampal gyrus, and inferior temporal and occipital cortex (Catani et al., 2002). The pAC fibers projecting to the inferior occipital cortex, and hence to multimodal/associative visual areas, develop earlier than the corpus callosum (Di Virgilio et al., 1999; Rockland and Pandya, 1986). In case of congenital callosal deficits or agenesis, the AC becomes strongly enlarged, sometimes up to four times its normal size, suggesting a possible compensatory role for this pathway in interhemispheric connectivity (Sarnat, 2008; Lassonde and Jeeves, 1994; van Meer et al., 2016). These adaptive changes involve multimodal/associative areas, like those connected by the pAC, that are crucial for cross-modal plasticity in blind subjects (Ortiz-Teran et al., 2016).

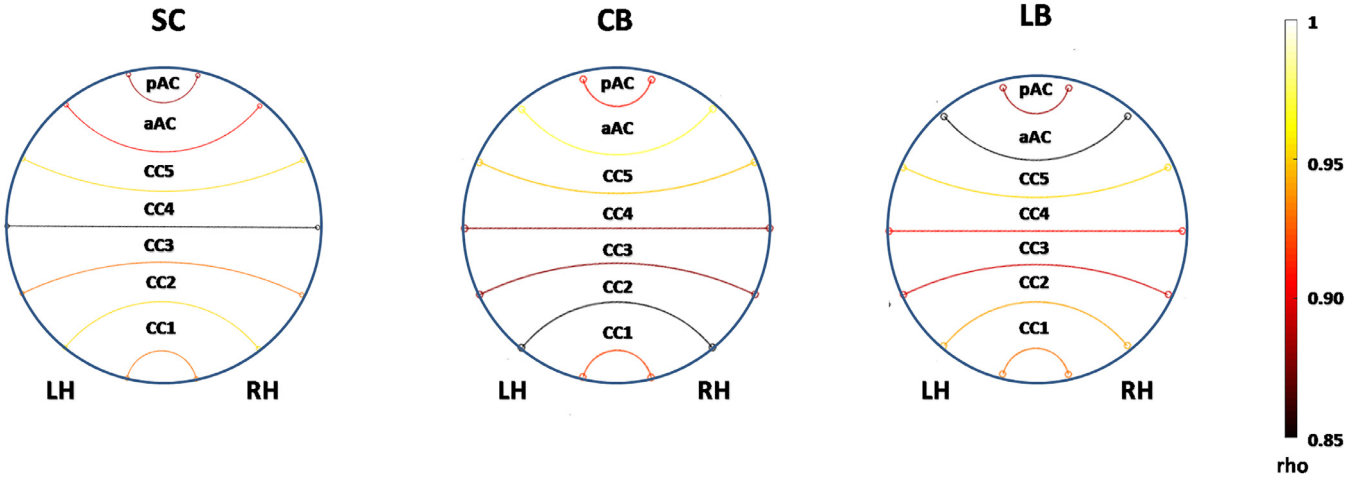

Fig. 4. *Tractography-driven functional connectivity analysis for homotopic cortical regions, connected through AC and CC streamlines.* Connectographs show mean Pearson correlation coefficients (rho) between homotopic cortical areas in the left and right hemisphere, conveyed by fibers passing through aAC, pAC, and the five callosal (CC1-5) subregions for SC, CB and LB.

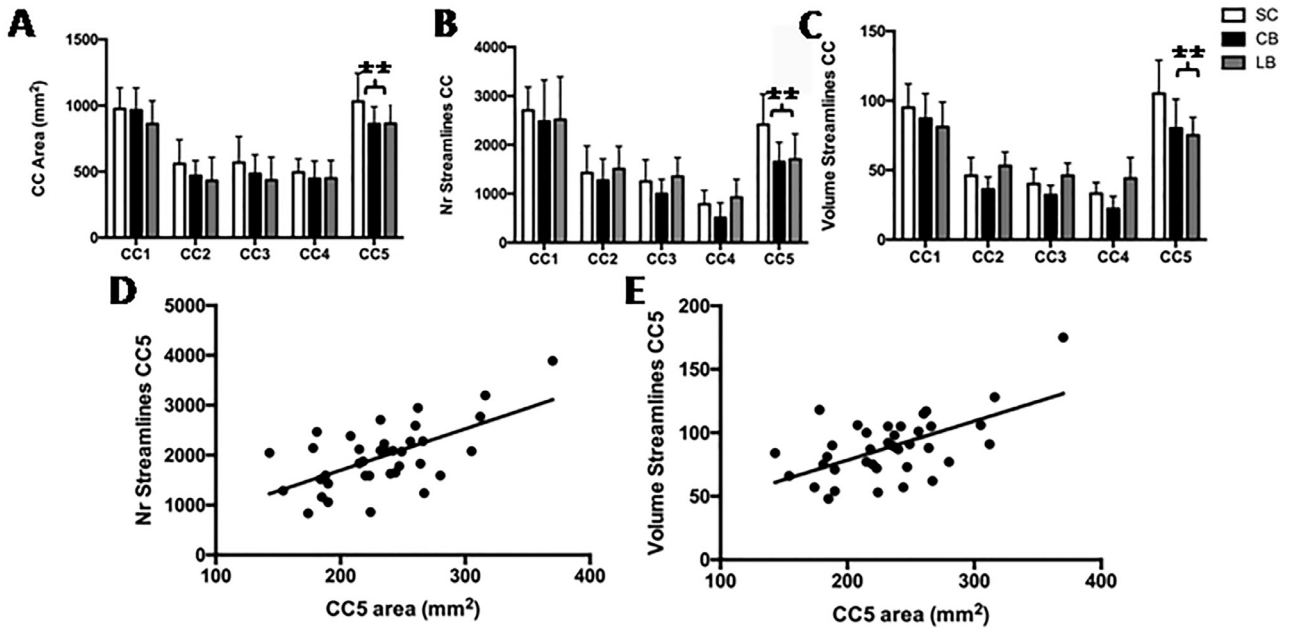

Fig. 5. *Tractography analysis of the five callosal segments*. (A)The area, (B) number of streamlines and (C) relative tract volumes for each of the five callosal subregions (upper part). Scatter plots for correlation analyses of CC5 surface area with number of streamlines (D) and tract volume (E) (lower part). **, $p < 0.01$.

Table 3
Tract-specific measurements and functional connectivity analysis of the five segments of the corpus callosum.

Segments	Measurements	SC&&(mean ± SD)	CB&&(mean ± SD)	LB&&(mean ± SD)	CB vs SC&&p value	LB vs SC&&p value	CB vs LB&&p value
Anterior	Streamlines	2705 ± 477	2483 ± 842	2515 ± 877	0.43	0.53	0.93
	Volume	95.53 ± 17.09	87.82 ± 18.07	82 ± 18.69	0.27	0.07	0.43
	FA	0.27 ± 0.03	0.27 ± 0.05	0.3 ± 0.05	0.75	0.15	0.13
	MD	0. 9 ± 0.05 x (10–3)	0.9 ± 0.1 x (10–3)	0.8 ± 0.09 x (10–3)	0.2	0.14	0.03
	AD	1 ± 0.05 x (10–3)	1 ± 0.09 x (10–3)	1 ± 0.07 x (10–3)	0.12	0.17	0.01
	Mean BOLD correlation	0.94 ± 0.04	0.92 ± 0.08	0.94 ± 0.06	0.41	0.99	0.47
Anterior mid-body	Streamlines	1425 ± 553	1270 ± 444	1509 ± 462	0.03	0.17	0.08
	Volume	46.79 ± 13.2	36.25 ± 9.93	53 ± 10.81	0.03	0.17	0.07
	FA	0.29 ± 0.04	0.29 ± 0.06	0.31 ± 0.06	0.87	0.26	0.42
	MD	0.8 ± 0.06 x (10–3)	0.9 ± 0.1 x (10–3)	0.8 ± 0.1 x (10–3)	0.91	0.17	0.32
	AD	1 ± 0.04 x (10–3)	1 ± 0.09 x (10–3)	1 ± 0.08 x (10–3)	0.93	0.14	0.22
	Mean BOLD correlation	0.96 ± 0.04	0.85 ± 0.21	0.95 ± 0.05	0.12	0.64	0.15
Posterior mid-body	Streamlines	1250 ± 446	999 ± 297	1353 ± 386	0.02	0.53	0.05
	Volume	40.36 ± 11.48	32.33 ± 7.11	46 ± 9.55	0.04	0.17	0.09
	FA	0.31 ± 0.04	0.3 ± 0.06	0.33 ± 0.07	0.85	0.3	0.29
	MD	0.8 ± 0.06 x (10–3)	0.8 ± 0.1 x (10–3)	0.8 ± 0.1 x (10–3)	0.73	0.08	0.22
	AD	1 ± 0.08 x (10–3)	1 ± 0.08 x (10–3)	1 ± 0.09 x (10–3)	0.68	0.07	0.2
	Mean BOLD correlation	0.94 ± 0.05	0.88 ± 0.18	0.91 ± 0.07	0.36	0.38	0.6
Isthmus	Streamlines	784 ± 283	507 ± 306	924 ± 372	0.02	0.31	0.008
	Volume	33.21 ± 8.54	22.94 ± 9.99	44 ± 15.58	0.01	0.92	0.01
	FA	0.3 ± 0.04	0.28 ± 0.06	0.35 ± 0.06	0.45	0.02	0.01
	MD	0.8 ± 0.09 x (10–3)	0.8 ± 0.1 x (10–3)	0.7 ± 0.1 x (10–3)	0.75	0.03	0.04
	AD	1 ± 0.07 x (10–3)	1 ± 0.1 x (10–3)	1 ± 0.1 x (10–3)	0.95	0.09	0.14
	Mean BOLD correlation	0.87 ± 0.12	0.88 ± 0.1	0.92 ± 0.05	0.85	0.39	0.26
Splenium	Streamlines	2415 ± 623	1653 ± 397	1706 ± 518	0.0009*	0.003*	0.79
	Volume	105.82 ± 24.22	80.83 ± 21.34	75 ± 13.34	0.003*	0.009*	0.45
	FA	0.35 ± 0.05	0.29 ± 0.07	0.35 ± 0.05	0.01	0.92	0.01
	MD	0.7 ± 0.07 x (10–3)	0.9 ± 0.1 x (10–3)	0.8 ± 0.1 x (10–3)	0.08	0.45	0.04
	AD	1 ± 0.05 x (10–3)	1 ± 0.09 x (10–3)	1 ± 0.1 x (10–3)	0.44	0.26	0.13
	Mean BOLD correlation	0.96 ± 0.04	0.95 ± 0.03	0.96 ± 0.02	0.87	0.53	0.36

Numbers are means ± SD. *Indicates values that survive Bonferroni correction for multiple comparisons. FA = fractional anisotropy; MD = mean diffusivity; AD = axial diffusivity.

Alterations of the splenium in congenital and late-onset blindness

There is a vast literature describing the multiple functions of the corpus callosum, ranging from interhemispheric transfer of sensory and motor information to the shaping of the lateralization of cognitive functions (Lepore et al., 1985; Zaidel and Iacoboni, 2003; Lassonde and Jeeves, 1994). The corpus callosum is undoubtedly the most important commissure not only by its sheer size, wealth of fibers and connections (Lamantia and Rakic, 1990), but also by its various functions that have been documented in a large series of studies in animal and human models of split-brain and callosal agenesis (Zaidel and Iacoboni, 2003; Lassonde and Jeeves, 1994). Although the corpus callosum is vulnerable to alterations in sensory inputs (Desgent and Ptito, 2012), it is capable of plasticity since manipulations of visual inputs lead to a strong re-arrangement of callosal projections (Innocenti and Frost, 1979; Ptito, 2003; Ptito and Boire, 2003).

We found a significant reduction of the splenium mid-sagittal area in both CB and LB participants. Considering that the splenium is primarily composed of fibers connecting visuo-spatial areas (Putnam et al., 2010), it is not surprising that this part was the most affected in blind individuals. Our finding of a significant reduction of the splenium in CB and LB is in line with other reports showing brain morphometric changes in this part of the corpus callosum in congenital (Ptitoet al., 2008; Leporéet al., 2010; Tomaiuolo et al., 2014) and late onset blindness (Qin et al., 2015; Shi et al., 2015; Reislev et al., 2016a). In the LB group, neuroplastic changes vary as a function of timing of onset of blindness and are most pronounced in individuals who became blind earlier in life (Noppeney, 2007; Jiang et al., 2009). The present study confirms our earlier results that the total surface area of the corpus callosum remains unchanged in CB (Tomaiuolo et al., 2014) and extends these by showing that the same holds true for LB. Contradictory findings have been reported for the isthmus and the posterior portion of the body that showed an enlargement in the study by Tomaiuolo et al. (2014), or the anterior portion of the corpus callosum (genu) that was reduced in a study by Leporé et al. (2010). Other studies failed to document changes in these callosal subregions. These seemingly contradictory results might be due to differences in the segmentation approach used (e.g., mid-sagittal plane vs. CC volume, or manual vs. semiautomatic technique), and sample size (12 CB in the current study compared to 28 in Tomaiuolo et al., 2014). Possibly, an even minimal difference in the brain tilting and regional subdivision can affect surface estimation due to the ratio between these small regions and the voxel size used ($1mm^3$).Moreover, the reduction in splenium volume, combined with a generalized change in callosal shape as reported elsewhere (Tomaiuolo et al., 2014; Ptito et al., 2008) could bias callosal subdivisions and measurements, unequally affecting different portion of CC, and following cortical projections.

The reduction of the splenium in both groups of blind subjects occurred concurrently with a significant decrease in the number of streamlines and tract volume crossing this region, but without changes in FA averaged along the tract. While some authors reported DWI parameters modifications in the corpus callosum using a ROI-based approach (Wang et al., 2013; Reislev et al., 2016b), only one other study described a reduced anatomical connectivity of the corpus callosum in CB but not in LB (Reislev et al., 2016a). The differences with the existing literature can be explained by differences in methodological approaches. When performing the analysis at the voxel level, reduced FA values in sections of the corpus callosum outside the splenium are found (Wang et al., 2013; Reislev et al., 2016b). The fact that we used a mean FA tract measure for each of the five callosal subregions could explain the absence of differences in the callosal fibers. Regarding the previous finding of reduced anatomical connectivity in the corpus callosum of CB subjects (Reislev et al., 2016a), the different tractography algorithm used (probabilistic vs spherical deconvolution) could explain these discrepancies. Nevertheless, another study comparing CB to SC reported a decreased structural connectivity between bilateral pericalcarine regions through the splenium (Shimony et al., 2006), supporting our result of a reduced number of connections between bilateral occipital cortices.

We were not able to identify alterations in functional connectivity in our blind subjects. Only one paper reported a reduced functional connectivity of the bilateral occipital cortices in CB, as measured by resting state fMRI (Liu et al., 2007). These results are in contrast with a more recent report (Ortiz-Téran et al., 2016) that described increased interconnectivity across multimodal integration areas and between unimodal regions and multimodal integration cortices in blind individuals. The differences with our findings may be explained by the fact that we did not apply an a priori occipital parcellation to identify regions of interest, but we considered all the cortical projections for each of the five callosal subregions, obtained using spherical deconvolution fiber tractography. Moreover, the DTI-derived cortical areas could be affected by the uncertainty associated with tractography methods that increases dramatically when approaching the cortex for the increased streamlines crossing points.

Conclusions

We show for the first time that the pAC, but not the aAC, undergoes compensatory neuroplastic changes in CB and LB. Our results further support the findings that the splenium, a structure primarily composed of fibers connecting the visual areas of the brain, is indeed sensitive to visual deprivation in both CB and LB. These data provide new insights into neuroplastic alterations of the commissural fiber system following blindness.

Ethical statement

None of the authors has any conflict of interest. Informed consent was obtained from all patients and the study was approved by the local ethical committee for the city of Copenhagen and Frederiksberg (Denmark).

CRediT authorship contribution statement

Carlo Cavaliere: Writing - original draft. **Marco Aiello:** Visualization, Formal analysis. **Andrea Soddu:** Formal analysis, Writing - review & editing. **Steven Laureys:** Formal analysis, Writing - review & editing. **Nina L Reislev:** Visualization. **Maurice Ptito:** Methodology, Formal analysis, Data curation, Writing - review & editing. **Ron Kupers:** Methodology, Formal analysis, Data curation, Writing - review & editing.

Declaration of Competing interest

None.

Acknowledgments

The study was supported by grants from the Lundbeck Foundation to RK and by the Harland Sanders chair in Visual Science to MP. AS was supported by the Natural Science and Engineering Research Council (NSERC) of Canada. The authors would like to thank Dr. Vladimir Fonov (McConnell Brain Imaging centre, Mc Gill University) for help with the segmentation of the corpus callosum.

Supplementary materials

Supplementary material associated with this article can be found, in the online version, at doi:10.1016/j.nicl.2019.102133.

References

Aiello, M., Salvatore, E., Cachia, A., Pappatà, S., Cavaliere, C., Prinster, A., et al., 2015. Relationship between simultaneously acquired resting-state regional cerebral glucose metabolism and functional MRI: a PET/MR hybrid scanner study. Neuroimage 113, 111–121.

Bavelier, D., Neville, H.J., 2002. Cross-modal plasticity: where and how? Nat. Rev. Neurosci. 3, 443–452.

Barr, M.S., Corballis, M.C., 2002. The role of the anterior commissure in callosal agenesis. Neuropsychology 16, 459–471.

Bayard, S., Gosselin, N., Robert, M., Lassonde, M., 2004. Inter- and intra-hemispheric processing of visual event-related potentials in the absence of the corpus callosum. J. Cognit. Neurosci. 16, 401–414.

Berman, N.E., Payne, B.R., 1983. Alterations in connections of the corpus callosum following convergent and divergent Strabismus. Brain Res. 274, 201–212.

Bermudez, P., Zatorre, R.J., 2001. Sexual dimorphism in the corpus callosum: methodological considerations in MRI morphometry. Neuroimage 6, 1121–1130.

Bock, A.S., Saenz, M., Tungaraza, R., Boynton, G.M., Bridge, H., Fine, I., 2013. Visual callosal topography in the absence of retinal input. Neuroimage 81, 325–334.

Bridge, H., Cowey, A., Ragge, N., Watkins, K., 2009. Imaging studies in congenital anophthalmia reveal preservation of brain architecture in 'visual' cortex. Brain 132, 3467–3480.

Brown, W.S., Jeeves, M.A., Dietrich, R., Burnison, D.S., 1999. Bilateral field advantage and evoked potential interhemispheric transmission in commissurotomy and callosal agenesis. Neuropsychologia 37, 1165–1180.

Catani, M., Howard, R.J., Pajevic, S., Jones, D.K., 2002. Virtual in vivo interactive dissection of white matter fasciculi in the human brain. Neuroimage 17, 77–94.

Catani, M., Robertsson, N., Beyh, A., Huynh, V., de Santiago Requejo, F., Howells, H., et al., 2017. Short parietal lobe connections of the human and monkey brain. Cortex 97, 339–357.

Cavaliere, C., Aiello, M., Di Perri, C., Amico, E., Martial, C., Thibaut, A., Laureys, S., Soddu, A., 2016. Functional connectivity substrates for tDCS response in minimally conscious state patients. Front. Cell. Neurosci. 10, 257. https://doi.org/10.3389/fncel.2016.00257.

Chao-Gan, Y., Yu-Feng, Z., 2010. DPARSF: a matlab toolbox for "pipeline" data analysis of resting-state fMRI. Front. Syst. Neurosci. 4, 13. https://doi.org/10.3389/fnsys.2010.00013.

Chebat, D.R., Chen, J.K., Schneider, F., Ptito, A., Kupers, R., Ptito, M., 2007. Alterations in right posterior hippocampus in early blind individuals. Neuroreport 18, 329–333.

Chen, Y., Tymofiyeva, O., Hess, C.P., Xu, D., 2015. Effects of rejecting diffusion directions on tensor-derived parameters. Neuroimage 109, 160–170.

Dejerine, J., 1895. Anatomie Des Centres Nerveux. Rueff, Paris.

Dell'Acqua, F., Simmons, A., Williams, S.C., Catani, M., 2013. Can spherical deconvolution provide more information than fiber orientations? hindrance modulated orientational anisotropy, a true-tract specific index to characterize white matter diffusion. Hum. Brain Mapp. 34, 2464–2483.

Desgent, S., Ptito, M., 2012. Cortical GABAergic interneurons in cross-modal plasticity following early blindness. Neural Plast., 590725. https://doi.org/10.1155/2012/590725.

Di Virgilio, G., Clarke, S., Pizzolato, G., Schaffner, T., 1999. Cortical regions contributing to the anterior commissure in man. Exp. Brain Res. 124, 1–7.

Elbert, T., Sterr, A., Rockstroh, B., Pantev, C., Müller, M.M., Taub, E., 2002. Expansion of the tonotopic area in the auditory cortex of the blind. J. Neurosci. 22, 9941–9944.

Fortin, M., Voss, P., Lord, C., Lassonde, M., Pruessner, J., Saint-Amour, D., et al., 2008. Wayfinding in the blind: larger hippocampal volume and supranormal spatial navigation. Brain 131, 2995–3005.

Friston, K.J., Frith, C.D., 1995. Schizophrenia: a disconnection syndrome? Clin. Neurosci. 3, 89–97.

Frost, D.O., Moy, Y.P., 1989. Effects of dark rearing on the development of visual callosal connections. Exp. Brain Res. 78, 203–213.

Giacosa, C., Karpati, F.J., Foster, N.E., Penhune, V.B., Hyde, K.L., 2016. Dance and music training have different effects on white matter diffusivity in sensorimotor pathways. Neuroimage 135, 273–286.

Guenot, M., 1998. Interhemispheric transfer and agenesis of the corpus callosum. Capacities and limitations of the anterior commissure. Neurochirurgie. 44, 113–115.

Hänggi, J., Koeneke, S., Bezzola, L., Jäncke, L., 2010. Structural neuroplasticity in the sensorimotor network of professional female ballet dancers. Hum. Brain Mapp. 31, 1196–1206.

Heine, L., Bahri, M.A., Cavaliere, C., et al., 2015. Prevalence of increases in functional connectivity in visual, somatosensory and language areas in congenital blindness. Front Neuroanatomy 9 (86). https://doi.org/10.3389/fnana.2015.00086.

Imfeld, A., Oechslin, M.S., Meyer, M., Loenneker, T., Jancke, L., 2009. White matter plasticity in the corticospinal tract of musicians: a diffusion tensor imaging study. Neuroimage 46, 600–607.

Innocenti, G.M., Frost, D.O., 1979. Effects of visual experience on the maturation of the efferent system to the corpus callosum. Nature 280, 231–234.

Jiang, J., Zhu, W., Shi, F., Liu, Y., Li, J., Qin, W., Li, K., Yu, C., Jiang, T., 2009. Thick visual cortex in the early blind. J. Neurosci. 29, 2205–2211.

Jones, D.K., Horsfield, M.A., Simmons, A., 1999. Optimal strategies for measuring diffusion in anisotropic systems by magnetic resonance imaging. Magn. Reson. Med. 42, 515–525.

Kupers, R., Pietrini, P., Ricciardi, E., Ptito, M., 2011. The nature of consciousness in the visually deprived brain. Front. Psychol. 2, 19. https://doi.org/10.3389/fpsyg.2011.00019.

Kupers, R., Ptito, M., 2014. Compensatory plasticity and cross-modal reorganization following early visual deprivation. Neurosci. Biobehav. Rev. 41C, 36–52.

Lamantia, A.S., Rakic, P., 1990. Cytological and quantitative characteristics of four cerebral commissures in the rhesus monkey. J. Comp. Neurol. 291, 520–537.

Lassonde, M., Jeeves, M.A., 1994. Callosal agenesis: A natural Split brain? Plenum, 1994, New York.

Leemans, A., Jones, D.K., 2009. The B–matrix must be rotated when correcting for subject motion in DTI data. Magn. Reson. Med. 61, 1336–1349.

Lepore, F., Ptito, M., Provençal, C., Bédard, S., Guillemot, J.P., 1985. Interhemispheric transfer of visual training in the split-brain cat: effects of the experimental setup. Can. J. Psychol. 39, 400–413.

Leporé, N., Voss, P., Lepore, F., Chou, Y.Y., Fortin, M., Gougoux, F., et al., 2010. Brain structure changes visualized in early- and late-onset blind subjects. Neuroimage 49, 134–140.

Levin, N., Dumoulin, S.O., Winawer, J., Dougherty, R.F., Wandell, B.A., 2010. Cortical maps and white matter tracts following long period of visual deprivation and retinal image restoration. Neuron 65, 21–31.

Liu, Y., Yu, C., Liang, M., et al., 2007. Whole brain functional connectivity in the early blind. Brain 130, 2085–2096.

Liu, L., Yuan, C., Ding, H., et al., 2017. Visual deprivation selectively reshapes the intrinsic functional architecture of the anterior insula subregions. Sci. Rep. 7, 45675. https://doi.org/10.1038/srep45675.

Livy, D.J., Schalomon, P.M., Roy, M., Zacharias, M.C., Pimenta, J., Lent, R., Wahlsten, D., 1997. Increased axon number in the anterior commissure of mice lacking a corpus callosum. Exp. Neurol. 146, 491–501.

Lund, R.D., Mitchell, D.E., 1979. The effect of dark-rearing on visual callosal connections of cats. Brain Res. 167, 172–175.

Mai, J., Paxinos, G., Voss, T., 1997. Atlas of the Human Brain, 3rd ed. Elsevier Academic Press, London.

Noppeney, U., 2007. The effects of visual deprivation on functional and structural organization of the human brain. Neurosci. Biobehav. Rev. 31, 1169–1180.

Ortiz-Terán, L., Ortiz, T., Perez, D.L., Aragón, J.I., Diez, I., Pascual-Leone, A., Sepulcre, J., 2016. Brain plasticity in blind subjects centralizes beyond the modal cortices. Front. Syst. Neurosci. 10, 61. https://doi.org/10.3389/fnsys.2016.00061.

Patel, M.D., Toussaint, N., Charles-Edwards, G.D., Lin, J.P., Batchelor, P.G., 2010. Distribution and fibre field similarity mapping of the human anterior commissure fibres by diffusion tensor imaging. MAGMA 23, 399–408.

Ptito, M., 2003. Functions of the corpus callosum as derived from split-chiasm studies in cats. In: Zaidel,, E., Iacoboni,, M. (Eds.), The Parallel Brain: The Cognitive Neuroscience of the Corpus Callosum. MIT Press, Cambridge, MA, pp. 139–153.

Ptito, M., Boire, D., 2003. Binocular input elimination and the reshaping of callosal connections. In: Zaidel, E., Iacoboni, M (Eds.), The Parallel brain: The Cognitive Neuroscience of the Corpus Callosum. MIT Press, Cambridge, MA, pp. 30–33.

Ptito, M., Lepore, F., 1983. Interocular transfer in cats with early callosal transection. Nature 301:bv/w2bnv 513-5.

Ptito, M., Schneider, F.C., Paulson, O.B., Kupers, R., 2008. Alterations of the visual pathways in congenital blindness. Exp. Brain Res. 187, 41–49.

Putnam, M.C., Steven, M.S., Doron, K.W., Riggall, A.C., Gazzaniga, M.S., 2010. Cortical projection topography of the human splenium: hemispheric asymmetry and individual differences. J. Cognit. Neurosci. 22, 1662–1669.

Qin, W., Xuan, Y., Liu, Y., Jiang, T., Yu, C., 2015. Functional connectivity density in congenitally and late blind subjects. Cereb. Cortex 25, 2507–2516.

Reich, D.S., Smith, S.A., Jones, C.K., Zackowski, K.M., van Zijl, P.C., Calabresi, P.A., Mori, S., 2006. Quantitative characterization of the corticospinal tract at 3T. AJNR Am. J. Neuroradiol. 27, 2168–2178.

Reislev, N.L., Dyrby, T.B., Siebner, H.R., Kupers, R., Ptito, M., 2016a. Simultaneous assessment of white matter changes in microstructure and connectedness in the blind brain. Neural Plast. 2016, 6029241. https://doi.org/10.1155/2016/6029241.

Reislev, N.L., Kupers, R., Siebner, H.R., Ptito, M., Dyrby, T.B., 2016b. Blindness alters the microstructure of the ventral but not the dorsal visual stream. Brain Struct. Funct. 221, 2891–2903.

Rockland, K.S., Pandya, D.N., 1986. Topography of occipital lobe commissural connections in the rhesus monkey. Brain Res. 365, 174–178.

Sarnat, H.B., 2008. Embryology and malformations of the forebrain commissures. In: Sarnat,, H.B, Curatolo,, P. (Eds.), Handbook of Clinical Neurology, Volume 87 (third series), Malformations of the Nervous System. Elsevier, Edinburgh, pp. 67–87.

Shi, J., Collignon, O., Xu, L., 2015. Impact of early and late visual deprivation on the structure of the corpus callosum: a study combining thickness profile with surface tensor-based morphometry. Neuroinformatics 13, 321–336.

Shimony, J.S., Burton, H., Epstein, A.A., McLaren, D.G., Sun, S.W., Snyder, A.Z., 2006. Diffusion tensor imaging reveals white matter reorganization in early blind humans. Cereb. Cortex 16, 1653–1661.

Stevens, A.A., Weaver, K.E., 2009. Functional characteristics of auditory cortex in the blind. Behav. Brain Res. 196, 134–138.

Tomaiuolo, F., Campana, S., Collins, D.L., Fonov, V.S., Ricciardi, E., Sartori, G., Pietrini, P., Kupers, R., Ptito, M., 2014. Morphometric changes of the corpus callosum in congenital blindness. PLoS One 9, e107871. https://doi.org/10.1371/journal.pone.0107871.

Tremblay, F.1., Ptito, M., Lepore, F., Miceli, D., Guillemot, J.P., 1987. Distribution of visual callosal projection neurons in the Siamese cat: an HRP study. J. Hirnforsch. 28, 491–503.

Van Meer, N., Houtman, A.C., Schuerbeek, P.V., Vamderhasselt, T., Milleret, C., Tusscher, M.P., 2016. Interhemispheric connections between the primary visual cortical areas via the anterior commissure in human callosal agenesis. Front. Syst. Neurosci. 10, 101. https://doi.org/10.3389/fnsys.2016.00101.

Wang, D., Qin, W., Liu, Y., Zhang, Y., Jiang, T., Yu, C., 2013. Altered white matter integrity in the congenital and late blind people. Neural Plast. 2013, 128236. https://

doi.org/10.1155/2013/128236.
Wedeen, V.J., Wang, R.P., Schmahmann, J.D., Benner, T., Tseng, W.Y., Dai, G., Pandya, D.N., Hagmann, P., D'Arceuil, H., de Crespigny, A.J., 2008. Diffusion spectrum magnetic resonance imaging (DSI) tractography of crossing fibers. Neuroimage 41, 1267–1277.
Witelson, S.F., 1989. Hand and sex differences in the isthmus and genu of the corpus callosum. A post-mortem morphological study. Brain 112, 799–835.
Yu, C., Shu, N., Li, J., Qin, W., Jiang, T., Li, K., 2007. Plasticity of the corticospinal tract in early blindness revealed by quantitative analysis of fractional anisotropy based on diffusion tensor tractography. Neuroimage 36, 411–417.
Zaidel, E., Iacoboni, M., 2003. Sensory-motor integration in the split-brain. In: Zaidel,, E., Iacoboni,, M. (Eds.), The Parallel Brain: The Cognitive Neuroscience of the Corpus Callosum. MIT Press, Cambridge, MA, pp. 319–336.
Zuo, X.-N., Xu, T., Jiang, L., Yang, Z., Cao, X.-Y., He, Y., et al., 2013. Toward reliable characterization of functional homogeneity in the human brain: preprocessing, scan duration, imaging resolution and computational space. Neuroimage 65, 374–386.